

Optical properties of rolled-up tubular microcavities from shaped nanomembranes

G. S. Huang (黄高山), S. Kiravittaya, V. A. Bolaños Quiñones, F. Ding (丁飞), M. Benyoucef, A. Rastelli, Y. F. Mei (梅永丰), and O. G. Schmidt

Citation: *Appl. Phys. Lett.* **94**, 141901 (2009); doi: 10.1063/1.3111813

View online: <https://doi.org/10.1063/1.3111813>

View Table of Contents: <http://aip.scitation.org/toc/apl/94/14>

Published by the [American Institute of Physics](#)

Articles you may be interested in

[Exceptional transport property in a rolled-up germanium tube](#)
Applied Physics Letters **110**, 112104 (2017); 10.1063/1.4978692

[Vertically aligned rolled-up SiO₂ optical microcavities in add-drop configuration](#)
Applied Physics Letters **102**, 251119 (2013); 10.1063/1.4812661

[Localized optical resonances in low refractive index rolled-up microtube cavity for liquid-core optofluidic detection](#)
Applied Physics Letters **101**, 151107 (2012); 10.1063/1.4758992

[System investigation of a rolled-up metamaterial optical hyperlens structure](#)
Applied Physics Letters **95**, 083104 (2009); 10.1063/1.3211115

[On-chip Si/SiO_x microtube refractometer](#)
Applied Physics Letters **93**, 094106 (2008); 10.1063/1.2978239

[Monolithically integrated self-rolled-up microtube-based vertical coupler for three-dimensional photonic integration](#)
Applied Physics Letters **107**, 031102 (2015); 10.1063/1.4927243



5 Electronic Measurement Pitfalls to Avoid

Get the whitepaper

Optical properties of rolled-up tubular microcavities from shaped nanomembranes

G. S. Huang (黄高山),^{1,a)} S. Kiravittaya,^{1,2} V. A. Bolaños Quiñones,¹ F. Ding (丁飞),^{1,2} M. Benyoucef,¹ A. Rastelli,¹ Y. F. Mei (梅永丰),^{1,a)} and O. G. Schmidt¹

¹Institute for Integrative Nanosciences, IFW Dresden, Helmholtzstr. 20, D-01069 Dresden, Germany

²Max-Planck-Institut für Festkörperforschung, Heisenbergstrasse 1, D-70569 Stuttgart, Germany

(Received 17 December 2008; accepted 9 February 2009; published online 6 April 2009)

Tubular optical microcavities have been fabricated by releasing prestressed SiO/SiO₂ bilayer nanomembranes from polymer sacrificial layers, and their geometrical structure is well controlled by defining the shape of nanomembranes via photolithography. Optical measurements at room temperature demonstrate that resonant modes of microtubular cavities rolled up from circular shapes can be tuned in peak energy and relative intensity along the tube axes compared to those from square patterns. The resonant modes shift to higher energy with decreasing number of tube wall rotations and thickness, which fits well to finite-difference time-domain simulations. Polarization resolved measurements of the resonant modes indicate that their polarization axes are parallel to the tube axis, independent of the polarization of the excitation laser. © 2009 American Institute of Physics. [DOI: 10.1063/1.3111813]

In recent years, optical microcavities have gained considerable interest because of their applications in optoelectronics and integrated optics.^{1,2} Optical microcavities of different materials have been investigated in the forms of microdisks,³ microspheres,^{4,5} or micropillars.⁶ By using a roll-up mechanism, micro-/nanotubular structures have been fabricated out of prestressed thin solid films.⁷⁻⁹ Several works have demonstrated the possibility to employ such rolled-up microtubes as optical microcavities.⁹⁻¹¹ However, due to distinct properties such as thin tube walls and spiral cross sections, it is important to further investigate optical properties of rolled-up tubular microcavities.¹² For example, an exact tailoring of the resonant modes in microcavities has been demonstrated, which shows light confinement along the tube axis, induced by a well-defined rolling edge.¹³ In this letter, rolled-up microcavity arrays are constructed by releasing prestressed SiO/SiO₂ bilayers on patterned photoresist layers.¹⁴ Photoluminescence (PL) measurements of these tubular microcavities exhibit optical resonant modes, while the visibility of the modes and peak positions can be tuned by varying the number of rotations of the tube wall. Good agreement is found between experimental results and simulations using the finite-difference time-domain (FDTD) method. The tubular microcavities proposed in this work may find applications in biosensing^{14,15} and optical frequency combs.¹⁶

The formation process of tubular microcavities is schematically displayed in Fig. 1(a). Briefly, a uniform $\sim 2 \mu\text{m}$ thick ARP-3510 photoresist (Allresist GmbH) layer on Si wafer was defined into squares and circles with various sizes by photolithography. The SiO/SiO₂ bilayer was deposited by e-beam evaporation employing angled deposition.^{9,14} Acetone was used to selectively remove the photoresist layer, releasing the active layer, and the intrinsic stress gradient existing in the bilayer caused the bilayer to self-assemble into a tubular microcavity.¹⁴ The morphologies of the

samples were investigated using a combination of scanning electron microscopy (SEM) (in Zeiss NVision40 workstation) and optical microscopy (Zeiss Axiotech vario). The optical properties were characterized by micro-PL spectroscopy at room temperature with an excitation line at 532 nm (20 μW).

Figure 1(b) shows optical microscopy images of microtube arrays formed on circular (left panel) and square (right panel) photoresist patterns. In both cases, the microtubes ($\sim 5.5 \mu\text{m}$ in diameter and 60 μm in length) arrange in a

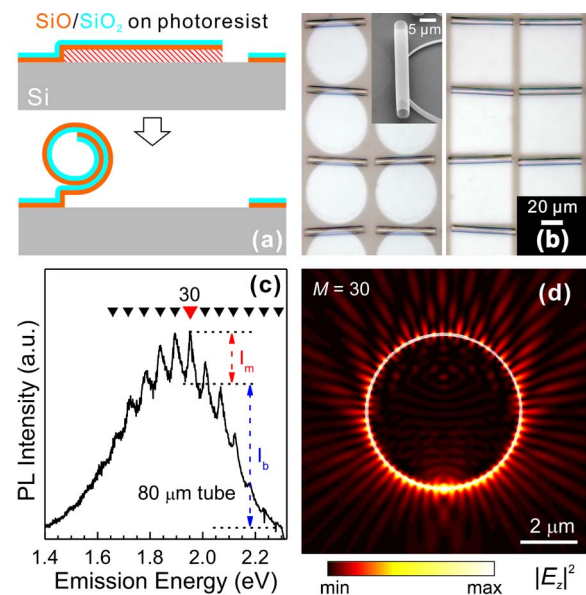


FIG. 1. (Color online) (a) Schematic diagram illustrating the fabrication process of rolled-up SiO/SiO₂ microtubes. (b) Optical microscope image of ordered microtube arrays from nanomembranes of different shapes: circles (left panel) and squares (right panel). The inset shows an SEM image of a microtube rolled up from a circular nanomembrane. Intensities of the mode ($M=30$) and the broad emission band are defined as I_m and I_b , respectively. The triangles indicate the mode positions obtained from the FDTD simulation. (d) Intensity pattern of the electric field for $M=30$ mode.

^{a)}Authors to whom correspondence should be addressed. Electronic addresses: g.huang@ifw-dresden.de and y.mei@ifw-dresden.de.

highly ordered manner and align into the same direction. This demonstrates that the employed approach enables us to roll up nanomembranes with different shapes and at the same time to control the orientations/positions of the microtubes. The number of rotations of the microtube rolled up from the circular geometry varies with the distance from the middle of the tube, thus allowing us to tailor the structure of the microtube.¹⁴ It is worth noting that the SEM image in Fig. 1(b) demonstrates a 2 μm gap between microtube and substrate, which efficiently suppresses the optical leakage and is important for optical devices. Figure 1(c) displays a PL spectrum from the middle of a microtube. Besides the broad emission band from the defect centers,¹⁷ a modulation of the PL spectrum is observed. This feature is ascribed to optical resonant modes, which originate from light of certain wavelengths circulating and interfering constructively in the tube wall.^{11,12} To support this interpretation, FDTD simulations were performed. The refractive indices used in the calculation are obtained from ellipsometry measurements, and the values are 1.55 and 1.45 for SiO and SiO₂ layers, respectively. The triangular symbols in Fig. 1(c) represent the mode positions derived from the simulation, which are in good agreement with the experiment. In addition, the electric field intensity pattern of a transverse-magnetic mode at ~ 1.95 eV (azimuthal number $M=30$) displayed in Fig. 1(d) indicates that the light indeed circulates in the tube wall and can be confined there. Nevertheless, the quality factor ($Q=E/\Delta E$, where E and ΔE are the position and width of the mode peak, respectively.) of these tubular microcavities is only ~ 100 , which is ascribed to losses due to the thin tube walls, absence of confinement along the tube axis, and other imperfections (roughness/voids).¹¹

The intensities and positions of the modes are sensitive to the structure of the microcavities.¹⁰ To quantitatively evaluate the dependence of mode intensity on structure, a series of PL spectra were collected along the axes of the microcavities rolled up from circular nanomembranes, and the relative intensities [I_m/I_b , see Fig. 1(c)] were calculated, as displayed in the lower insets of Figs. 2(a) and 2(b). The relative intensities reach their maximum at the middle of the tube, where the number of rotations, and hence wall thickness, is maximum. On the other hand, in the regions near the ends, the thinner tube walls weaken the light confinement and modes can no longer be observed. This is not the case in the microcavities rolled up from square nanomembranes, where the geometric structure is the same along the tube axis, so that the relative intensities [a typical result is displayed as the square in Fig. 2(a)] and peak positions (not shown) stay almost constant. Since the tube wall consists of a tightly rolled nanomembrane, the number of rotations along the axes of microcavities rolled up from circular nanomembranes can easily be calculated. The relation between relative intensities and number of rotations are displayed in Figs. 2(a) and 2(b). An interesting phenomenon is that modes become visible at ~ 2.7 rotations in the 60 μm tube while a larger number of rotations (~ 3.8 rotations) is required in the 80 μm microtube. This difference may possibly be due to the more compact tube wall in the shorter tube or the axial confinement of the light.¹³

In addition to the change of relative intensity, the microcavity structure has significant influence on the mode positions. Figure 3(a) shows the PL spectra measured at different positions on an 80 μm microtube along its axis. Obviously,

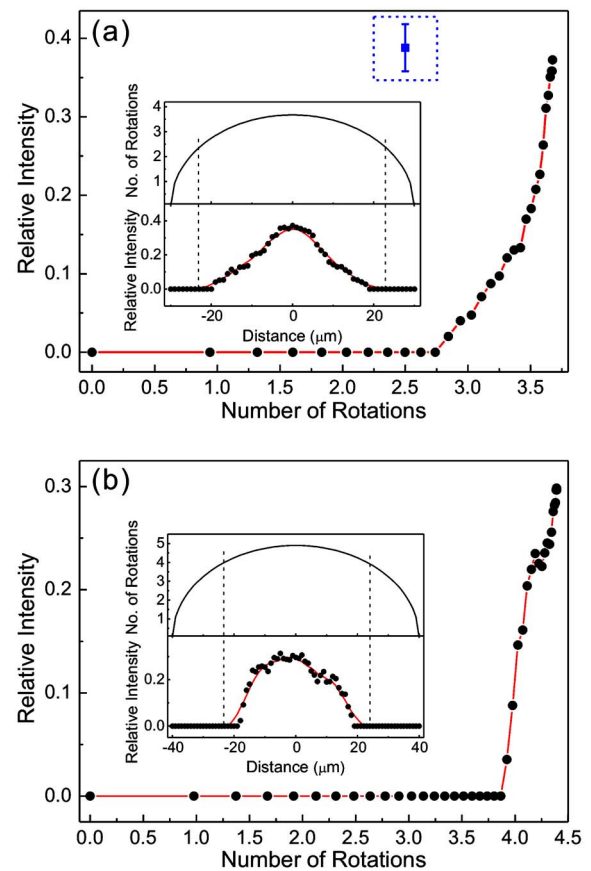


FIG. 2. (Color online) (a) Circles display the relative intensity of a resonant mode (with $M=29$) of a microtube rolled up from a circular nanomembrane with diameter of 60 μm as a function of the number of tube wall rotations. The solid line is a guide to the eye. The square represents the relative intensity of the resonant mode of a typical microtube rolled up from a square nanomembrane with size of 60 μm . The insets show the number of tube wall rotations (upper) and relative intensities of the resonant mode (lower) as a function of the distance from the middle of the tube. The solid line in the lower inset is a guide to the eye. (b) Results of the microtube from circular nanomembrane with diameter of 80 μm ($M=30$).

the resonant modes shift continuously to higher energy when moving from the middle to the end of the microtube. Similar results were also obtained from the 60 μm microtube [see circular symbols in Fig. 3(b) and its inset]. To understand this shift qualitatively, we consider the cross section at each position of a tubular microcavity as a circular waveguide.¹⁸ To obtain constructive interference for light traveling inside the tube walls, the periodic boundary condition $n_{\text{eff}}\pi d = M\lambda$ should be satisfied, where n_{eff} is the effective refractive index, d is the diameter of the microtube, and λ is the wavelength. With increasing distance from the middle of the tube, the number of rotations (i.e., the tube wall thickness) decreases and shortens the path of the light circulating inside the circular waveguide, which directly leads to a decrease of n_{eff} .¹⁰ As a consequence, the mode shifts to shorter wavelengths (higher energies) to satisfy the boundary condition. The quantitative analysis of the shift is obtained by FDTD simulations, which are displayed as dashed lines in Fig. 3(b) and its inset, and describe very well the experimental results.

To further investigate the optical properties of tubular microcavities, we have performed polarization dependent PL measurements on a microtube. The circular symbols in Fig. 4 show the relative intensity as a function of the linear polar-

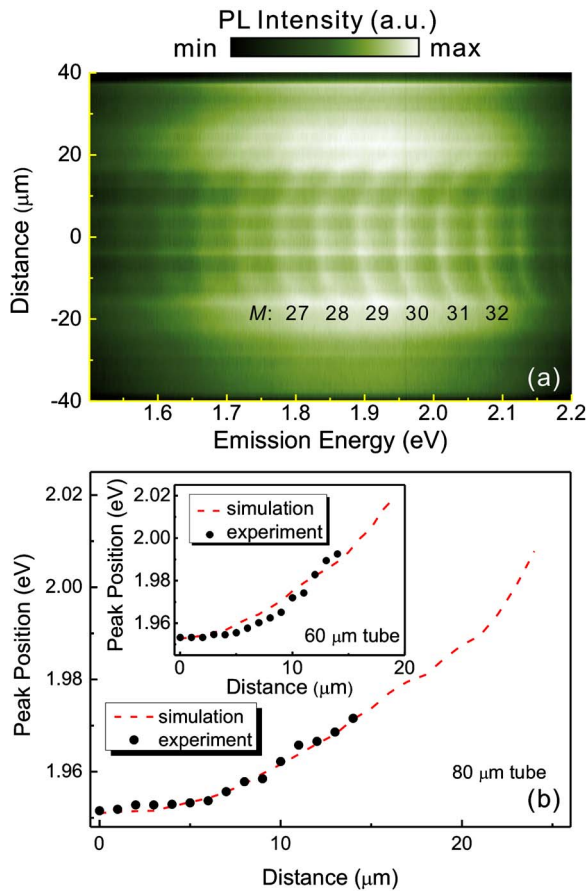


FIG. 3. (Color online) (a) Color coded PL intensity as a function of emission energy and the distance from the middle of an 80 μm microtube. (b) The circles show the experimental result of peak position ($M=30$) as a function of the distance (80 μm microtube). The result from the FDTD simulation is given by the dashed line. The inset shows the experiment and simulation results of the resonant mode ($M=29$) from a 60 μm microtube.

ization angle of the emitted light with respect to the tube axis. A cosine dependence is apparent, and no optical mode can be observed when the polarization axis is perpendicular to the tube axis. This indicates that only the light with polarization axis parallel to the tube axis can circulate in the tube wall. We also changed the polarization angle of the excitation laser, however, no polarization dependence is observed, as illustrated in the inset of Fig. 4. Due to the amorphous nature of the nanomembrane, the isotropic light emission from the defect centers is reasonable.

In summary, we have prepared tubular optical microcavities by releasing prestressed nanomembranes with different shapes from polymer layers, and the geometrical structure of the microcavities can be easily controlled by photolithography. Optically resonant modes are observed, and the mode positions correlate with the structural properties of the microcavities, in good agreement with FDTD simulations. The polarization dependence of the modes implies that light polarized parallel to the tube axis can easily propagate in the tubular microcavity, whereas the emission properties are independent of the polarization of the excitation laser.

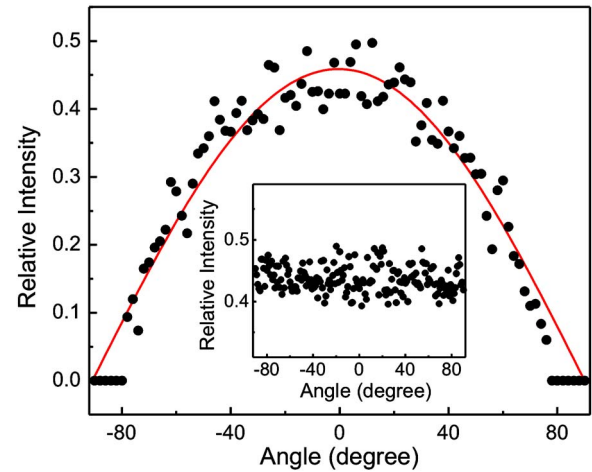


FIG. 4. (Color online) (a) Relative intensity of the resonant mode ($M=30$) as a function of the linear polarization angle of the emitted light with respect to the tube axis (circles). The solid line is the cosine fit. The inset shows the relative intensity of the resonant mode (with $M=30$) as a function of the polarization angle of the excitation laser with respect to the tube axis (circles), and only the emitted light polarized parallel to the tube axis was collected.

We are grateful for experimental help by Dr. Ingolf Mönch, Ronny Engelhard, Emica Coric, Dr. Juliane Gabel, Johannes David Plumhof, Dr. Hong Seok Lee, and Santosh Kumar.

- ¹D. K. Armani, T. J. Kippenberg, S. M. Spillane, and K. J. Vahala, *Nature (London)* **421**, 925 (2003).
- ²K. J. Vahala, *Nature (London)* **424**, 839 (2003).
- ³S. L. McCall, A. F. J. Levi, R. E. Slusher, S. J. Pearton, and R. A. Logan, *Appl. Phys. Lett.* **60**, 289 (1992).
- ⁴J. C. Knight, N. Dubreuil, V. Sandoghdar, J. Hare, V. Lefèvre-Seguin, J. M. Raimond, and S. Haroche, *Opt. Lett.* **20**, 1515 (1995).
- ⁵S. M. Spillane, T. J. Kippenberg, and K. J. Vahala, *Nature (London)* **415**, 621 (2002).
- ⁶J. M. Gérard, D. Barrier, J. Y. Marzin, R. Kuszelewicz, L. Manin, E. Costard, V. Thierry-Mieg, and T. Rivera, *Appl. Phys. Lett.* **69**, 449 (1996).
- ⁷V. Ya. Prinz, V. A. Seleznev, A. K. Gutakovskiy, A. V. Chehovskiy, V. V. Preobrazhenskii, M. A. Putyato, and T. A. Gavrilova, *Physica E (Amsterdam)* **6**, 828 (2000).
- ⁸O. G. Schmidt and K. Eberl, *Nature (London)* **410**, 168 (2001).
- ⁹Y. F. Mei, G. S. Huang, A. A. Solovlev, E. Bermúdez Ureña, I. Mönch, F. Ding, T. Reindl, R. K. Y. Fu, P. K. Chu, and O. G. Schmidt, *Adv. Mater. (Weinheim, Ger.)* **20**, 4085 (2008).
- ¹⁰T. Kipp, H. Welsch, Ch. Strelow, Ch. Heyn, and D. Heitmann, *Phys. Rev. Lett.* **96**, 077403 (2006).
- ¹¹R. Songmuang, A. Rastelli, S. Mendach, and O. G. Schmidt, *Appl. Phys. Lett.* **90**, 091905 (2007).
- ¹²M. Hosoda and T. Shigaki, *Appl. Phys. Lett.* **90**, 181107 (2007).
- ¹³Ch. Strelow, H. Rehberg, C. M. Schultz, H. Welsch, Ch. Heyn, D. Heitmann, and T. Kipp, *Phys. Rev. Lett.* **101**, 127403 (2008).
- ¹⁴G. S. Huang, Y. F. Mei, D. J. Thurmer, E. Coric, and O. G. Schmidt, *Lab Chip* **9**, 263 (2009).
- ¹⁵A. Bernardi, S. Kiravittaya, A. Rastelli, R. Songmuang, D. J. Thurmer, M. Benyoucef, and O. G. Schmidt, *Appl. Phys. Lett.* **93**, 094106 (2008).
- ¹⁶A. A. Savchenkov, A. B. Matsko, V. S. Ilchenko, I. Solomatine, D. Seidel, and L. Maleki, *Phys. Rev. Lett.* **101**, 093902 (2008).
- ¹⁷L. X. Yi, J. Heitmann, R. Scholz, and M. Zacharias, *Appl. Phys. Lett.* **81**, 4248 (2002) and references therein.
- ¹⁸Ch. Strelow, C. M. Schultz, H. Rehberg, H. Welsch, Ch. Heyn, D. Heitmann, and T. Kipp, *Phys. Rev. B* **76**, 045303 (2007).